KINETICS OF SURFACE OXIDATION OF METALS

AND ALLOYS DETERMINED BY SOLID ELECTROLYTE TECHNIQUES

Final Report (June, 1970)

by

G. R. Fitterer
C. D. Cassler
E. E. Mild

Prepared for

NATIONAL AERONAUTICS AND SPACE ADMINISTRATION

NASA GRANT NGR-39-011-067

R. E. Oldrieve, Project Manager
I. Zaplatinski, Research Advisor

NASA Lewis Research Center
Cleveland, Ohio 44135

Center for the Study of Thermodynamic Properties of Materials
Metallurgical and Materials Engineering Department
University of Pittsburgh, Pittsburgh, Pa. 15213

KINETICS OF SURFACE OXIDATION OF METALS

AND ALLOYS DETERMINED BY SOLID ELECTROLYTE TECHNIQUES

Final Report (June, 1970)

by

G. R. Fitterer
C. D. Cassler
E. E. Mild

Prepared for

NATIONAL AERONAUTICS AND SPACE ADMINISTRATION

NASA GRANT NGR-39-011-067

Center for the Study of Thermodynamic Properties of Materials
Metallurgical and Materials Engineering Department
University of Pittsburgh, Pittsburgh, Pa. 15213

TABLE OF CONTENTS

FOREWORD

This is the final report on this project which has been supported on NASA Grant NGR 39-011-067 with the objective of exploring and developing a new solid electrolyte technique for the determination of the mechanism and kinetics of oxidation of metals and alloys.

As will be shown excellent data were obtained in the case of iron oxidation but certain difficulties were encountered in the non-ferrous metals and alloys. However, one of the major difficulties was solved and the method which resulted is unique in that it not only provides kinetic data regarding oxidation but also indicates which oxide is forming at any given instant.

The method should be developed further since much important data can be obtained regarding the mechanism of oxidation by this method.

Report Submitted: June 1970

G. R. Fitterer
Principal Investigator

SUMMARY

This study of the solid electrolyte technique for determining the oxidation characteristics of metals and alloys has verified and extended the work of Tare and Schmalzried.[11] In fact, it has been shown that when the cell is properly prepared and manipulated, this technique provides both thermodynamic and kinetic data with surprising accuracy.

Time was not available to develop this procedure to the rapid and routine technique of which it is capable. However, methods for analysis of data from this cell have been devised and special thermodynamic treatments have resulted in very remarkable checks on data obtained by other methods.

This technique as modified and extended is a highly significant advancement and it is hoped that it will be continued somewhere to its ultimate usefulness.

A STUDY OF THE KINETICS OF THE SURFACE OXIDATION OF METALS AND ALLOYS BY SOLID ELECTROLYTE TECHNIQUES

INTRODUCTION

The much referred to development of solid electrolyte techniques by Kiukkola and Wagner[1] has nucleated a vast amount of metallurgical research of various types.

Investigations of this nature have established the free energies of various oxides,[1][2][3][4] and alloy phase boundaries.[5][6][7][8] Also, the diffusion rates of oxygen in solid[9] and liquid[10] metals have been recorded in the 10-12 years following the initial publication. Recently, solid electrolyte techniques for the study of the kinetics of high temperature reactions have been developed. Rickert's[9] research in this field is well known.

The work about to be described is an extension of the interesting technique suggested by Tare and Schmalzried[11] for the study of the kinetics of oxidation of solid metals and alloys. As shown schematically in Figure 1, the cell used in their work consisted of an electrolyte disc, on one side of which is pressed a metal foil of known thickness. A gaseous mixture of CO_2 and CO is directed against the metal foil and oxygen or air on the opposite side of the electrolyte serves as the reference state. Platinum leads and thermocouples permit one to measure the changes in the cell voltage during the oxidation of the metal at the selected temperature.

Figure 2 according to Tare and Schmalzried, schematically illustrates the trend of the cell potential with time. Prior to heating to the experimental
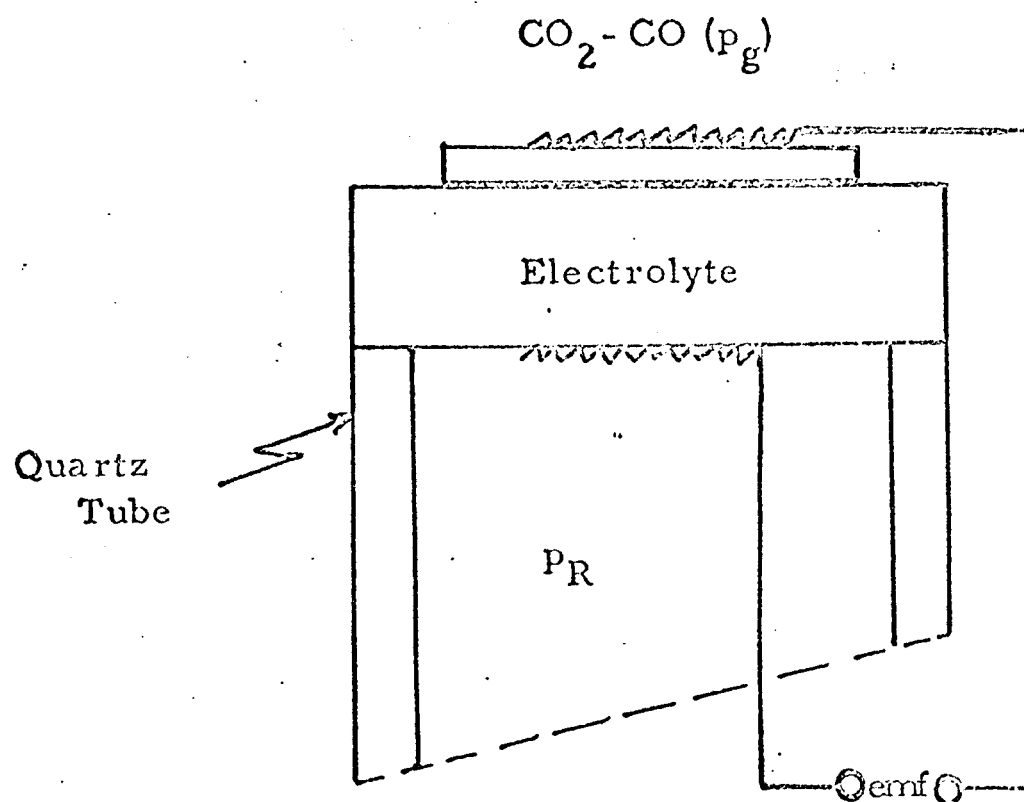
$$CO_2 - CO \ (p_g)$$

Electrolyte

Quartz
Tube

P_R

emf

Figure 1. Schematic Design of The Tare and Schmalzried[11] Solid
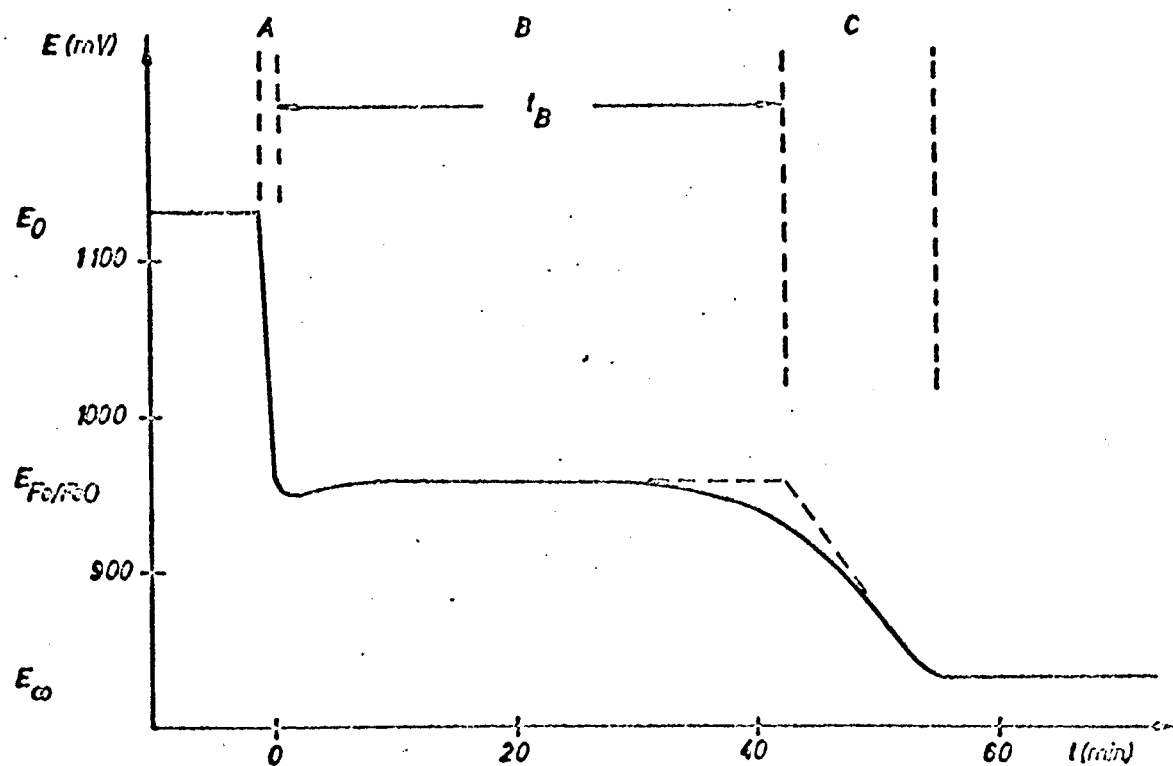Electrolyte Cell

Figure 2. Trends in Cell Voltage During Oxidation of Iron to Wüstite Tare and Schmalzried[11]

temperature, a voltage (E^o) is imposed against the cell so as to just prevent oxidation. Also, the CO_2/CO ratio is held slightly on the reducing side during heating. When thermal equilibrium has been attained, the gas ratio is suddenly changed to the desired level. Thus, during the initial period indicated as A in the figure, oxygen is adsorbed on the surface; and as in the case of the oxidation of iron, diffuses into the foil until the formation of wüstite is nucleated at the low point of the curve. Wüstite continues to form until the entire foil is transformed to oxide (i. e. , in period-B) after which the emf drops to a lower value (period-C) depending upon the oxygen differential. By means of this technique, a linear reaction rate constant for the oxidation of iron to wüstite was determined by these authors.

This investigation has been organized into two phases. Phase I has involved an attempt to duplicate the Tare and Schmalzried experimental procedure and data for the oxidation of iron.

Phase II has been directed toward the determination, if possible, of the oxidation characteristics of the more refractory metals and alloys by this same procedure.

The major objective of the entire project has been directed towards the evaluation of this technique as a more rapid method for determining the oxidation rates of metals than the usual micro-balance procedure or the weight gain methods.

PHASE I THE OXIDATION OF IRON

The problems involving the oxidation of iron have long been of great interest to many investigators. Some of the peculiarities of the reactions involved were complicated by the fact that three oxides, FeO, Fe_3O_4, and Fe_2O_3 exist and that any one or all may form during a given experiment. Further, it was realized by early investigators that "FeO" was not a stoichometric compound but was an iron deficient oxide which was given the name of Wüstite and also the symbol, Fe_xO.

Probably the most thorough investigation of the Wüstite field of the iron-oxygen system was made by Darken and Gurry.[12] Their studies established the phase boundaries of the system, as shown in Figure 3. The experimental method involved the suspension of a strip of slightly oxidized iron in a furnace with a known temperature gradient. A constant CO_2-CO mixture was passed through the furnace and in about an hour the oxidized specimen was removed, after first raising it to a cool part of the furnace where no reaction would take place. The oxides were then analyzed and studied along the length of the specimen. Knowledge of the temperature at each longitudinal position of the furnace and the variation in the analysis of the oxide film established the phase boundaries.

It was found by these investigators, as well as by many others later, that reactions of iron with oxygen are very sensitive to temperature changes, as well as to slight variations in oxygen pressure, as shown by the dotted lines in Figure 3. Thus, considerable care must be taken in any such experiments so as to accurately control all parameters.
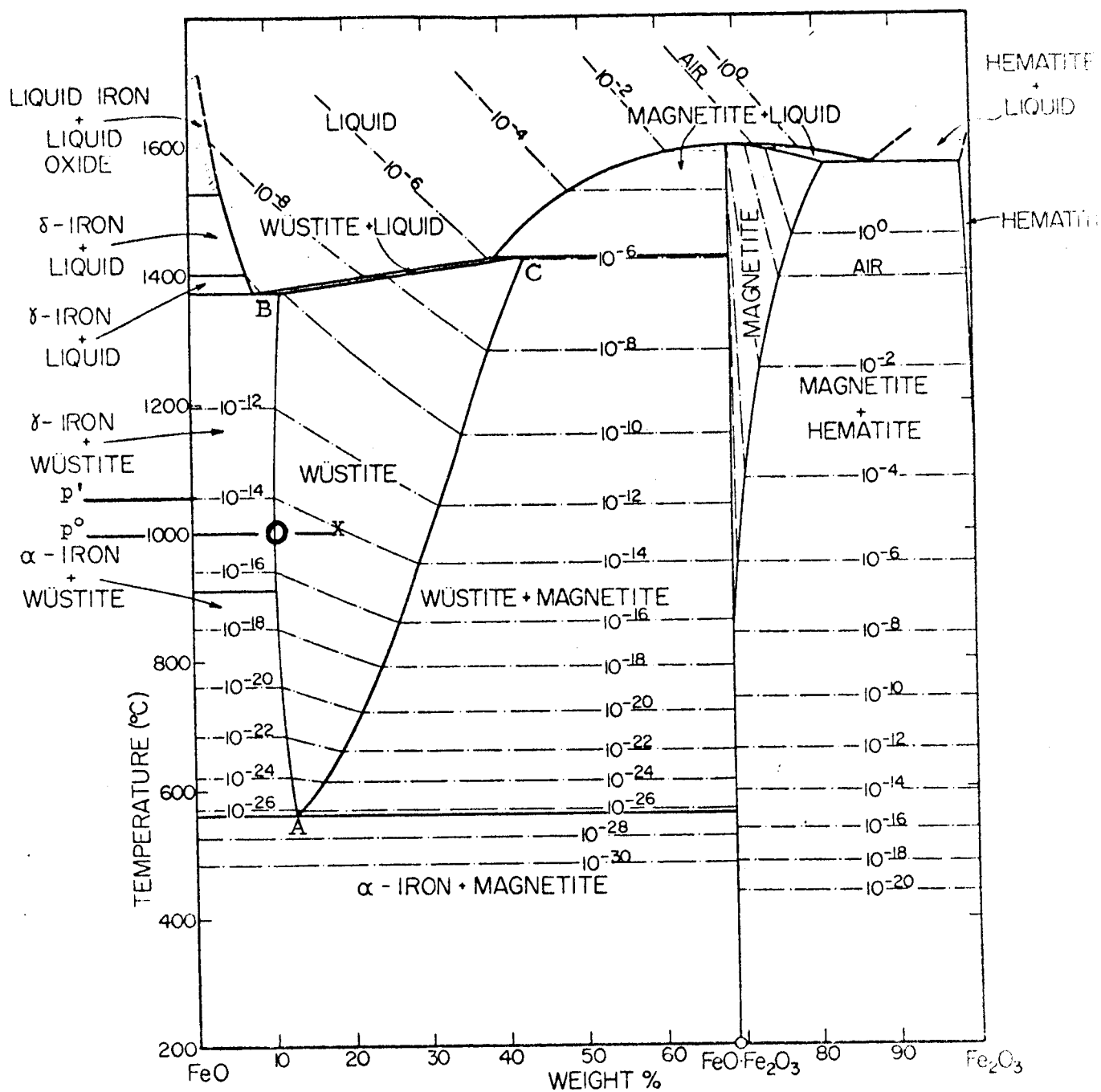
Figure 3   The FeO - Fe$_2$O$_3$ System according to Darken and Gurry[5]

Numerous investigators have also been interested in the determination of the rate of oxidation of iron under various conditions. Some techniques involved the change of weight of bulk specimens, whereas, others were concerned with the determination of the linear oxidation of thin foils when only one surface was exposed to the oxidizing medium. In general, it has been agreed that the reaction rate is linear for iron foils up to at least four or five mils in thickness. The current work extends this range.

EXPERIMENTAL TECHNIQUE AND CALIBRATION OF THE CELL

The cell used in the current work is shown in Figure 4. It is designed with three distinct electrical circuits. Circuit A-B is similar to the Tare and Schmalzried concept, and it is through this circuit that the changes in the cell voltage were measured during the oxidation of the metal foil.

The second circuit (i. e. , A-C) is designed to give the basic cell voltage, without the metal foil   The reaction involved is

$$CO + 1/2 \ O_{2 \text{(air)}} = CO_2 \ \text{-----------------------(1)}$$
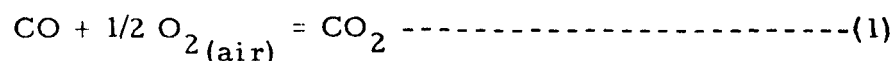
Inasmuch as the standard free energy of this reaction is well known, a family of curves, as shown in Figure 5, may be calculated in accordance with the van't Hoff isotherm:

$$\triangle G_R = -neF \quad \triangle G_1^o + RT \ln J \ \text{-----------------(2)}$$

$$e = \text{the cell voltage}$$

$$n = 2$$

$$F = 23,066 \text{ cal/volt or the Faraday equivalent}$$

Note: In all cases here-in-after the value of the reaction free energy will be considered to be related to the cell voltage since $\triangle G_R = -neF$.
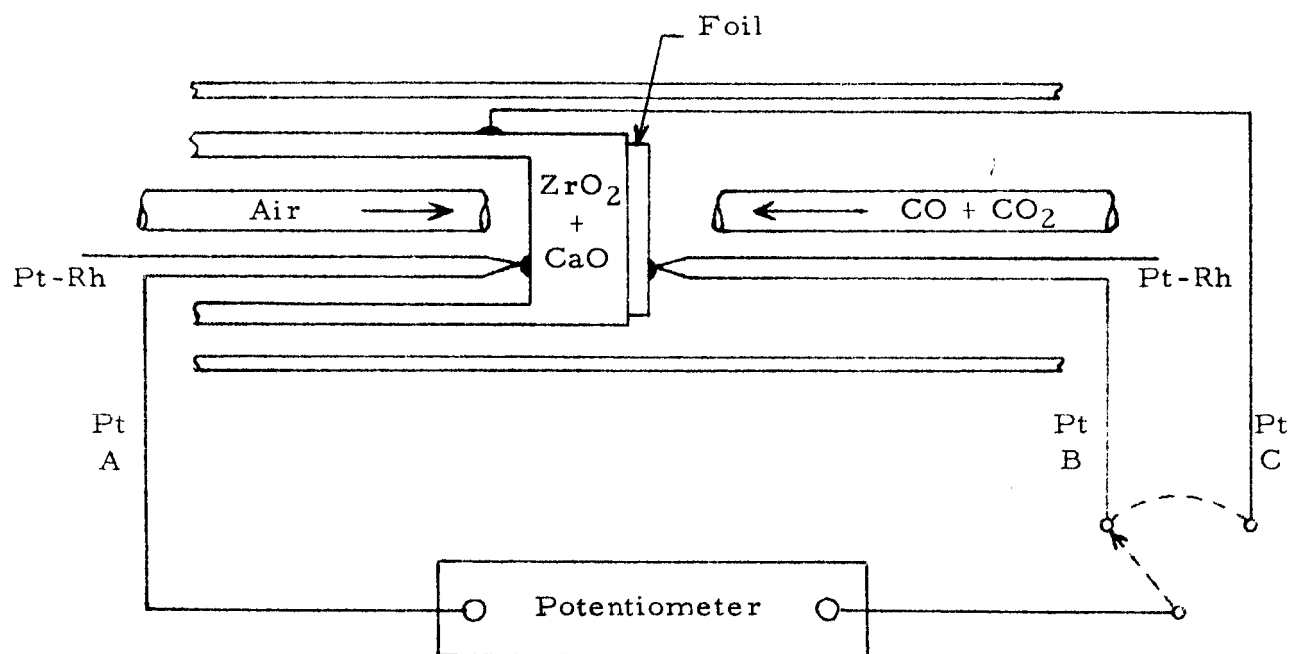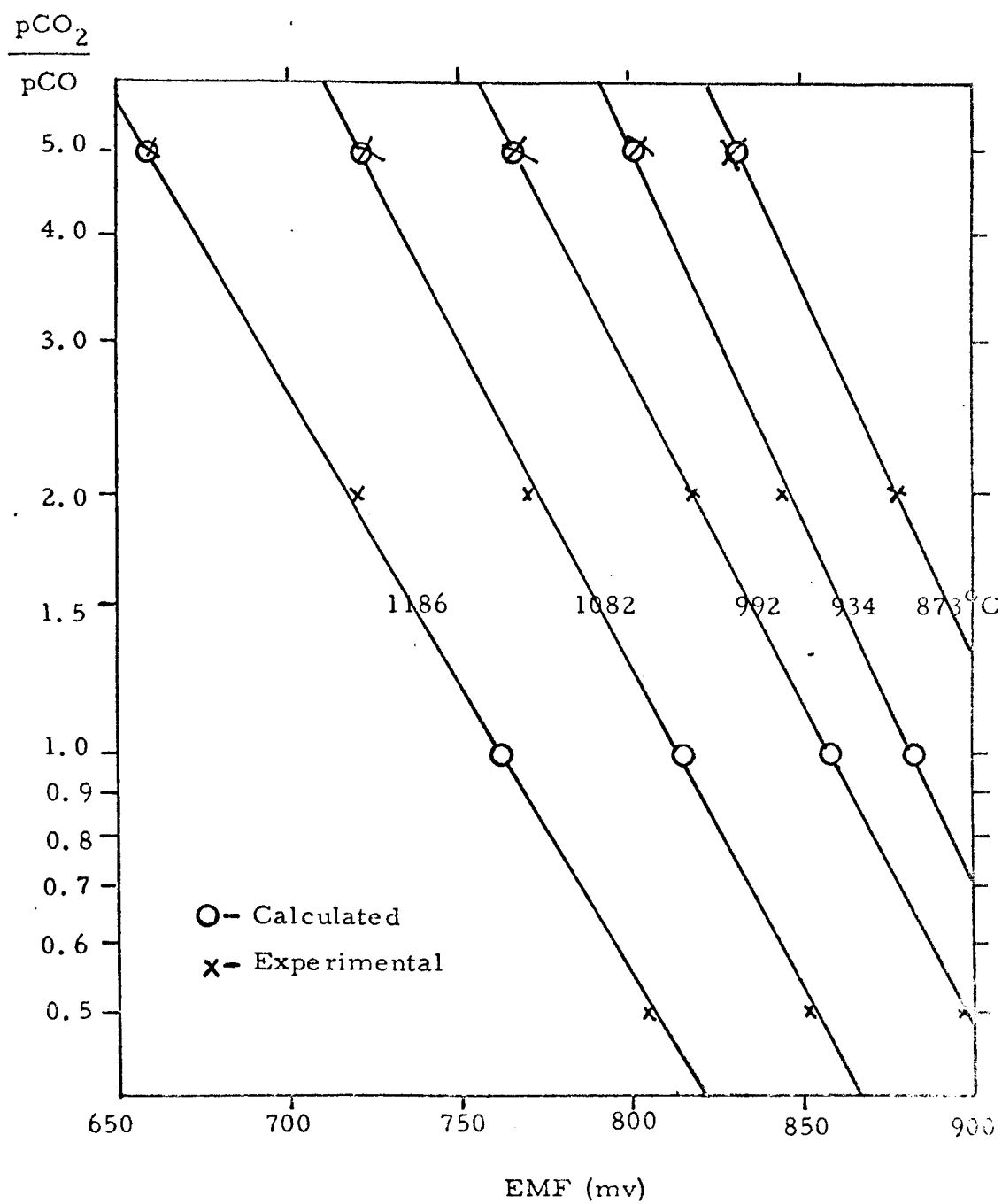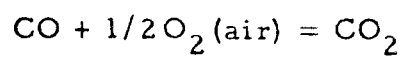
Figure 4   Experimental Apparatus (schematic)

Figure 5.   Calibration of The Solid Electrolyte Cell for The Reaction:

$$CO + 1/2 O_2 (air) = CO_2$$

$$\triangle G^{\circ} = -67,500 + 20.75T \text{ according to Kubaschewski,}$$
Evans and Alcock[13]

$$R = 1.986 \text{ cal}/^{\circ}K$$

$$T = {}^{\circ}K$$

$$J = pCO_2/pCO \sqrt{pO_2} \text{ where } pO_2 = 0.21 \text{ at. (air). Thus,}$$

J expresses the experimental non-equilibrium concentrations.

Preliminary tests were made using circuit A-C at various temperatures from 873 to $1186^{\circ}C$ and with CO_2/CO ratios as indicated in the figure. As shown, the experimental data correlate quite satisfactorily with the thermo-dynamically calculated lines. The maximum deviation of these experimental values from the calculated lines is less than 1%. Later, circuit A-C was used as a reference to check the cell behavior with metal foil during the experiments. Sudden alterations of the CO_2/CO ratio resulted in corresponding responses in the cell voltage within less than 15 seconds at all potential levels.

Sample Preparation   A billet of (99.99 + %) iron powder was prepared from iron carbonyl by Magnetics, Inc. of Butler, Pennsylvania. This billet was then rolled at the University to 0.100 inch strip at $2200^{\circ}F$ and returned to Magnetics, Inc. where it was cold reduced to (0.0043", 0.004" and 0.0004" thick) foils on a Sendzimer planetary mill. Some of the carbonyl iron billet material was also sliced and polished down to various thicknesses so as to extend the experimental data to heavier foil.

All samples were recrystallization annealed in hydrogen, then washed and cleaned with acetone prior to the oxidation experiments. The rolled material presented different types of surfaces and grain orientations than the samples which had been polished down from bulk specimens.

The cell of Figure 4 was also provided with a third electrical circuit which is not shown in the figure. This circuit was used to impose the (DC) back potential at the start of each experiment so as to prevent oxidation until the experimental temperatures had been attained. Further, the initial CO_2/CO ratio was adjusted at the start to a point which was very slightly on the reducing side according to prior thermodynamic calculations.

As in the Tare and Schmalzried procedure, the imposed potential was next removed and the CO_2/CO ratio was quickly adjusted to the desired experimental level. The temperature was also held at a constant level throughout each experiment. The cell voltage varied according to the oxidation trends during a given experiment in a manner similar to that in Figure 2.

Instrumentation   The cell voltage was recorded on a Honeywell, Electronic-1' which was backed up with a constant voltage source so that the instrument only recorded the top 100 millivolts during any given experiment. This insured that the cell emf was measured potentiometrically at all times.

A Honeywell Precision Rubicon Potentiometer was used to measure temperatures periodically throughout a given experiment.

Specially calibrated Manostat flow meters were used to adjust the CO_2/CO ratio throughout all experiments.

EXPERIMENTAL RESULTS

The experiments were designed to provide several "families" of curves which would represent the trends in the oxidation of iron under various conditions.

The variables which were scheduled in these experiments are:

1. The temperature (i.e., 900, 1000, and $1100^{\circ}C$)

2. The CO_2/CO ratios (i.e., 0.5, 1.0, 2.0, and 5.0)

3. As shown in Table 1, the foil thickness varied in ten steps from 0.0004" to 0.0096"

The three curves shown in Figure 6 are condensed reproductions of experimental curves and are typical of all of those obtained in the oxidation of iron. At an operating temperature of $900 \, ^{\circ}C$ and a CO_2/CO ratio of 2/1, the trends are similar and vary only because of the thickness of the foil. In each case, the initial CO_2/CO ratio was held at 0.35 as the samples were heated to the experimental temperature.

When the gas ratio was changed to 2/1, the emf dropped (as at Point-B) until the formation of wüstite was nucleated, then the voltage rose to the Point-C, as shown in the figure. All three of the C-values or peak voltages are within less than 1% of the calculated voltage for the formation of wüstite under these conditions.

These curves all differ from the Tare and Schmalzried schematic curve of Figure 2, because in these experiments the voltage started to drop as soon as the foil had been oxidized completely to wüstite. This continued in every case until the basic cell voltage for the formation of CO_2 was reached, as in Figure 5. It is assumed that at Point-C, the oxide film was saturated and had become so inactive, it merely served as an electrical contact for Reaction-1. Experimental data for all tests are given in Table 1.

The curves in Figure 6 are identifiable in Table 1 as tests numbered 1, 4, and 9.
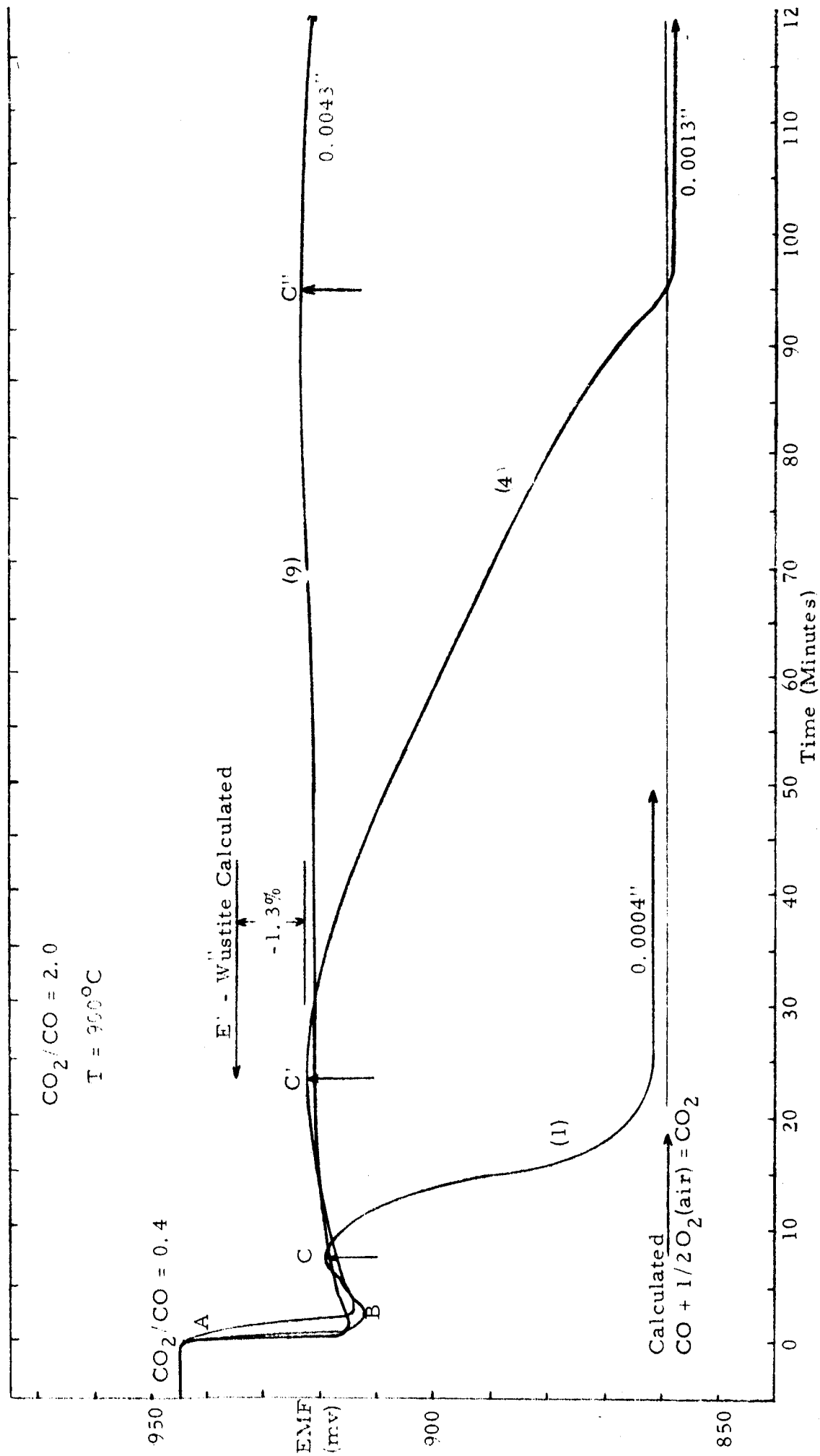
Figure 6 Typical Curves Showing Effects of Foil Thickness on Oxidation Rate of Iron

13

Table $\underline{1}$ -- Experimental Data
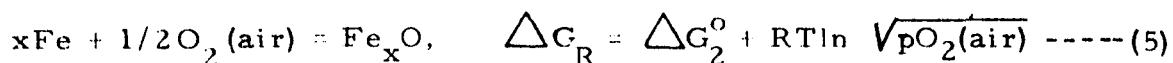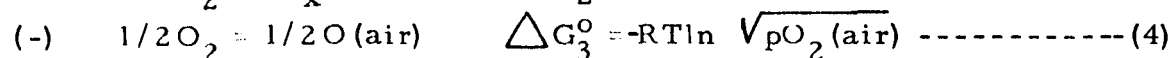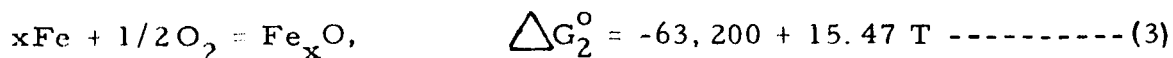
Test No.	Temp. (%C)	Foil Thickness (mils)	CO_2/CO Ratio	Time to Reach Peak (Min.)	E^o (Volts)	E' (Peak) (Volts)	$k_1 \times 10^{-8}$ $(\text{sec}^{-1}\text{cm}^{-2})$
1	900	0.4	2.0	6.0	0.938	0.918	0.862
2	900	0.4	5.0	6.5	0.945	0.895	2.00
3	900	1.0	5.0	22.0	0.948	0.916	0.935
4	900	1.3	2.0	23.0	0.950	0.923	0.970
5	900	1.3	5.0	22.5	0.943	0.870	2.79
6	900	1.3	5.0	24.5	0.935	0.862	2.48
7	900	4.0	2.0	70.0	0.948	0.921	1.00
8	900	4.0	5.0	68.0	0.940	0.901	1.52
9	900	4.3	2.0	95.0	0.943	0.923	0.582
10	900	4.3	5.0	75.0	0.943	0.900	1.59
11	1000	0.4	0.5	6.5	0.907	0.890	0.700
12	1000	0.4	0.5	3.5	0.906	0.889	1.28
13	1000	0.4	1.0	2.0	0.902	0.883	2.55
14	1000	0.4	1.0	4.0	0.906	0.890	1.07
15	1000	0.4	1.0	2.0	0.908	0.900	1.06
16	1000	0.4	1.0	3.0	0.918	0.900	1.58
17	1000	0.4	2.0	2.0	0.916	0.898	2.37
18	1000	0.4	2.0	2.0	0.904	0.876	3.76
19	1000	0.4	5.0	2.0	0.906	0.885	2.82
20	1000	0.4	5.0	2.0	0.902	0.868	4.60
21	1000	1.3	2.0	8.5	0.914	0.893	2.12
22	1000	1.3	5.0	5.0	0.905	0.873	5.58
23	1000	1.3	5.0	5.0	0.916	0.891	4.05
24	1000	4.0	2.0	24.5	0.913	0.900	1.41
25	1000	4.0	5.0	20.0	0.904	0.880	3.22
26	1000	4.0	5.0	18.5	0.920	0.900	2.84
27	1000	4.3	2.0	25.0	0.905	0.893	1.37
28	1000	4.3	5.0	20.0	0.905	0.883	3.16
29	1000	5.0	5.0	19.0	0.906	0.888	3.14
30	1000	5.5	5.0	20.5	0.908	0.895	2.31
31	1000	6.9	5.0	30.0	0.906	0.893	1.98
32	1000	8.2	5.0	37.0	0.906	0.896	1.47
33	1000	8.5	5.0	39.5	0.914	0.898	2.24
34	1000	9.5	5.0	45.0	0.909	0.888	2.94
35	1000	9.6	5.0	51.5	0.910	0.889	2.61
36	1100	0.4	1.0	1.5	0.877	0.862	2.73
37	1100	0.4	2.0	0.5	0.860	0.837	12.9
38	1100	0.4	5.0	0.5	0.864	0.817	26.5

In these studies, the time from the start of the oxidation to the peaks of the voltage curves (i.e., from points A to C of Figure 6) was selected as the total time for the oxidation of the foil. These time periods have been plotted against the thickness of the foil in Figure 7. Here, the effects of temperature and CO_2/CO ratio are clearly shown and it is apparent that the oxidation of iron under these conditions is linear for foils up to 0.0096" thickness. The variation in temperature is more effective than changes in CO_2/CO ratios within these ranges.

No attempt was made in this work to determine any variations in stoichiometry of the wüstite (i.e., the value of x in Fe_xO). This had been studied in considerable detail by Rizzo[14] using coulometric titration with solid electrolyte cells. It was assumed that the oxide in any given experiment did not deviate much from the composition designated by line A-B of Figure 3 for a given temperature.

THERMODYNAMIC CALCULATIONS

In this experimental system, two reactions are taking place simultaneously and both of these contribute to the cell potential. One of these involves the oxidation of iron with the reaction being referred to air as the standard state for oxygen. The second reaction involves the formation of CO_2 from CO and oxygen and this also is referred to air as the reference state.

$$xFe + 1/2\,O_2 = Fe_xO, \qquad \Delta G_2^o = -63,200 + 15.47\,T \quad \text{---------} (3)$$

$$(-) \quad 1/2\,O_2 = 1/2\,O\,(air) \qquad \Delta G_3^o = -RT\ln \sqrt{pO_2}\,(air) \quad \text{-----------} (4)$$

$$xFe + 1/2\,O_2\,(air) = Fe_xO, \qquad \Delta G_R = \Delta G_2^o + RT\ln \sqrt{pO_2}(air) \quad \text{-----} (5)$$
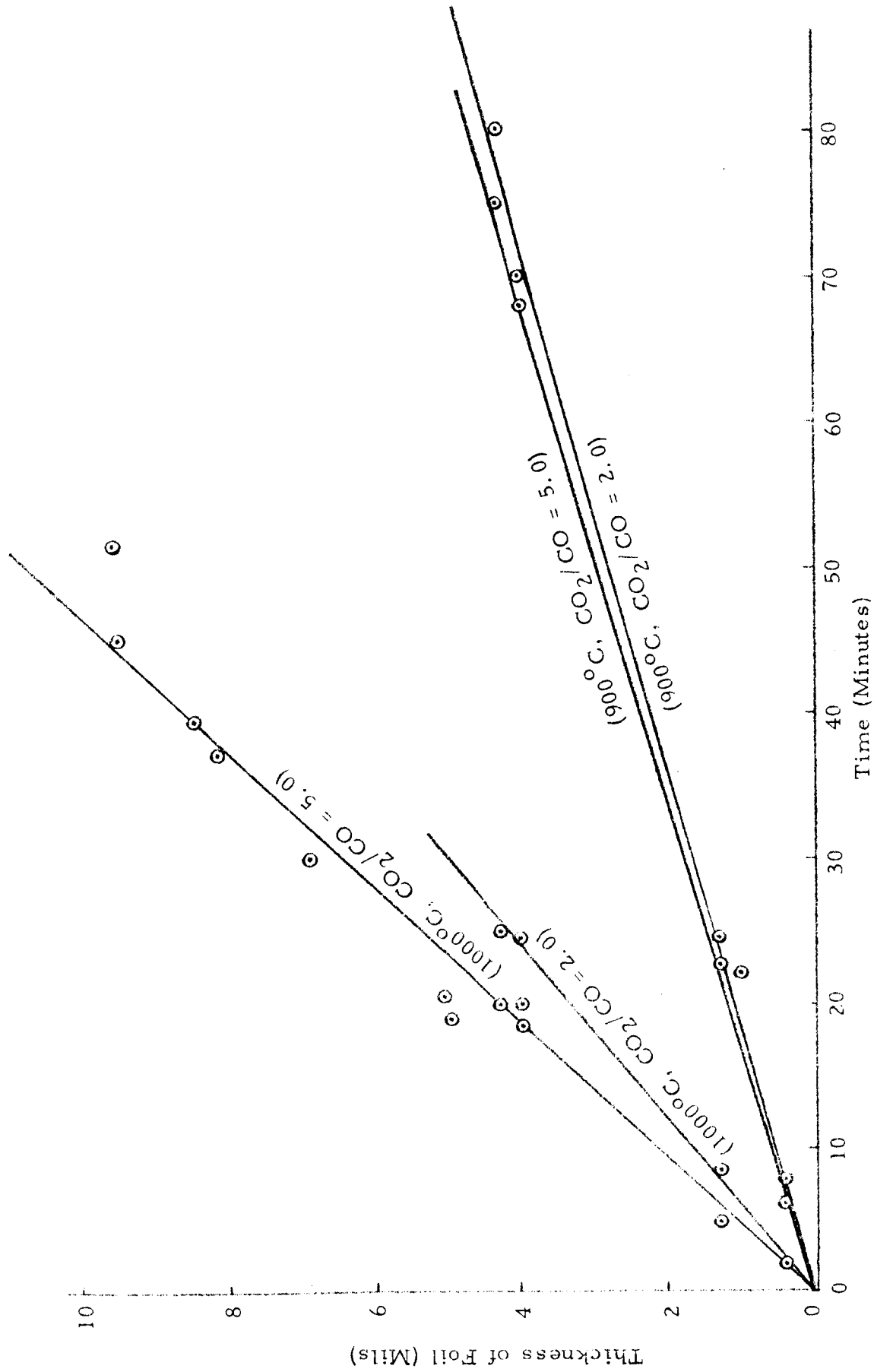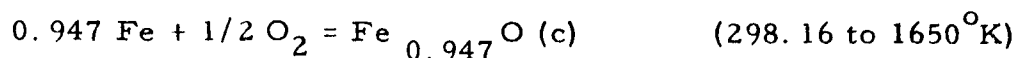
Figure 7   Thickness of Foil vs. Time to Reach "The Peak Voltage, E'

The $\triangle G_2^o$ values were obtained from Humphrey, King and Kelly[15] for the reaction:

$$0.947\ Fe + 1/2\ O_2 = Fe_{0.947}O\ (c) \qquad (298.16\ to\ 1650^oK)$$

In this experimental system, the reaction occurs under dynamic conditions which involve a constant flow of a CO_2 and CO mixture at a pre-set ratio. This reaction provides the oxygen for the oxidation of iron, so that according to the van't Hoff isotherm,

$$\triangle G_R = \triangle G_2^o + RT\ln \sqrt{pO_2\ (air)} + RT\ln \frac{pCO_2}{pCO\ \sqrt{pO_2\ (air)}}$$

$$or \quad \triangle G_R = \triangle G_2^o + RT\ln \frac{pCO_2}{pCO} \qquad \text{------------------(6)}$$

As shown in the Annual Report (10/23/68), the values obtained at the various experimental temperatures and gas ratios correlated quite well with values calculated from Equation 6.

In this experimental technique, the CO_2/CO mixture provides a source of oxygen at a given partial pressure which may be calculated from the temperature and the gas ratio being used. With this information, one may predict the extent of the wüstite reaction. If a ratio of CO_2/CO is being used which will produce an equilibrium pO_2 for the temperature level, the reaction will cease at the phase boundary indicated by line A-B in Figure 3.

If on the other hand, the partial pressure of oxygen is higher than the equilibrium level for the specified temperature, the wüstite will increase in oxygen content with a subsequent decrease in the x value of Fe_xO. This trend will proceed across the wüstite area of Figure 3 from line A-B toward line A-C until equilibrium is reached at a given temperature. For example, if at 1000^oC

a partial pressure of oxygen of $p^1 = 10^{-14}$ is used, equilibrium will be established at point-x of Figure 3. The increase in the oxygen content of wüstite to an extent that magnetite starts to form, requires a considerably higher CO_2/CO ratio.

In order to form any magnetite, the pO_2 must be increased to as much as 10^{-12} at this temperature. In order to accomplish this, the CO_2/CO ratio must be increased from 0.555 to 11.3.

Some indications were obtained in these experiments to verify these concepts. However, the porosity of the wüstite film under these conditions resulted in difficulty in reaching the magnetite region. No difficulty was encountered due to porosity, however, in any of the experiments terminating in equilibrium at the wüstite phase boundary.

KINETICS AND THE DETERMINATION OF THE RATE CONSTANT

In a cell of this type, the cell potential is a function of the reaction free energy as expressed in Equation-2. The reaction free energy in turn is a function of the dissociation pressure of the oxide in contact with the metal and the oxygen pressure in the gas phase which is determined by the CO_2/CO ratio at the experimental temperature with air as the reference.

In their study of the kinetics of oxidation of iron, Tare and Schmalzried[11] used a modified relationship suggested by Kubayaki and Wagner.[16] The time period selected in their work was the length of the plateau or B-section of their curves (Figure 2).

$$k = \frac{\Theta \cdot d_{Fe}}{t \cdot M(1-x)} \left[pCO_2 \left(1 - \frac{pCO}{pCO_2} \left(\frac{pCO_2}{pCO} \right) Fe/FeO \right) \right]^{-1}$$

where:
Θ = foil thickness (cm)
d = density of iron
t = time (seconds)
M = Atomic Weight of iron
$1-x$ = Composition $Fe_{(1-x)}O$ in equilibrium with iron

This relationship was also used by Pettit and Wagner[17] in a somewhat different form to describe a weight-gain study of the oxidation of iron.

In the current work, the rate constant was related to the time required for the cell voltage to change from the initial voltage at the start to that at point-C which was assumed to indicate the complete oxidation of the foil. As shown in Figure 6, no true voltage plateau region was indicated in the recordings of this work except when low CO_2/CO ratios were used at low temperatures. Even in these cases, however, the "plateau" was not entirely flat and a peak voltage was evident.

In this work, the rate constant was determined from the following equation:

$$k = \frac{\Theta d}{tM} \ln \frac{E^O}{E^O - \Delta E} \quad \text{------------------------------------} \quad (7)$$

where:
Θ = foil thickness (cm)
d = density of iron
t = time (seconds)
M = Atomic Weight of iron
E^O = Equilibrium electrode potential
ΔE = the difference between the experimental (E') and the equilibrium potential (E^O)

$\triangle E^o$ is related to the equilibrium oxygen pressure at the metal-oxide

surface and E' is related to the oxygen pressure at the gas-oxide surface.

This approach to the problem is similar to that proposed by Taylor[18]

for reactions in which one of the reactants was being consumed. In this case,

the iron is progressively transformed to oxide.

In the temperature range of 850-975°C, Tare and Schmalzried reported

an average rate constant of 3.5×10^{-8}. In this work at 900 and 1000°C, an

average of thirty five experiments indicates a rate constant of 2.38×10^{-8}.

Grabke[19] using electrical resistance measurements and radioactive tracer

techniques indicated specific rate constants of 1.59×10^{-9} and 1.81×10^{-9},

respectively, at 800°C.

Recent correspondence from H. Schmalzried indicated concurrence

in the rate constant reported in the current work and also indicated that this

is "essentially the value obtained by Dr. Bohnenkamp at the Max-Planck-Institut

fur Eisenforschung at Düsseldorf" in recent but unpublished work.

Forward Reaction Rates   Edmiston and Grace[20] reported an activation

energy of 27,400 calories for the reduction of wüstite with hydrogen in this

temperature range.

Their values were determined by calculations of the forward and

backward reaction rates by a method suggested by Prigogine, Outer and Herbo[21]

and developed further by others.[22][23]

This procedure was investigated in the current work as a second method

for the calculation of the activation energy. This method also is based on the

van't Hoff isotherm.

From the mass-action law, it is recognized that the equilibrium constant is a combination of the forward and backward rate constants, k_f and k_b. For example, in the reaction for the reduction of wüstite with hydrogen,

$$Fe_xO + H_2 \underset{k_b}{\overset{k_f}{\rightleftarrows}} x\,Fe + H_2O\ (g) \ \text{------------------------} \ (8)$$
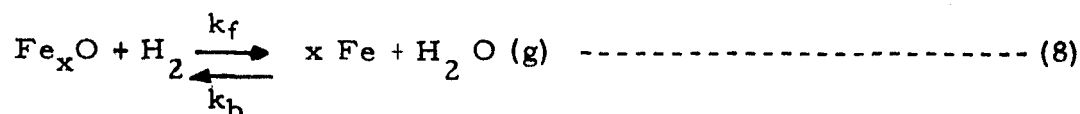
where the forward rate is, $R_f = k_f\,P_{H_2O}$ and the reverse rate is, $R_b = k_b\,P_{H_2O}$

The relationship between the reaction and the standard free energy values at any temperature may be expressed in terms of the partial pressures of the two gases according to the isotherm

$$\triangle G_R - \triangle G^o = RT\ln J \ \text{and}$$

$$\frac{R_f}{R_b} = \left(\frac{k_f}{k_b}\right)\left(\frac{P_{H_2}}{P_{H_2O}}\right) = \frac{K^e}{J}\ \exp\ -\left(\frac{\triangle G^o}{RT}\right) \ \text{------} (9)$$

At equilibrium, of course, $J=K$ and the forward and backward rates are equivalent. As shown by Edmiston and Grace, when this is expanded with a Taylor series, the higher order terms are neglected, and the derivatives evaluated at zero. The expression then reduces to

$$R_f - R_b = -R_b\ (\triangle G/RT) \ \text{----------------------------} (10)$$

When the over-all reaction rate $(R_f - R_b)$ is plotted against $-\triangle G/RT$, the slope of the line is numerically equal to the back reaction rate, (R_b). This then permits the calculation of the forward reaction rate.

R_f values for the current reaction were next calculated from the experimental data and these values were substituted in an Arrhenius type equation as follows:

$$\frac{d \ln R_f}{dT} = \frac{Q^*}{RT^2}$$, where Q^* is the activation energy and

$$\log R_f = \log A' - \frac{Q^*}{4.575T}$$ -------------------------------(11)

Values for $\log R_f$ were plotted against $\frac{10^4}{T}$, and from this plot,

the slope of the line was found to give an activation energy of 38,720 calories.

The averages of these points were plotted on an expanded scale in Figure 8, and

from this, the values for Equation -10 were obtained, i.e.,

$$\log R_f = 2.8 - \frac{38,720}{4.575T}$$ ------------------------------(12)

The average experimental values for $\log k$ were also plotted against $\frac{10^4}{T}$

where it is shown that this line is parallel to the $\log R_f$ line but has an intercept

of $\log k = \log 1$ or zero and,

$$\log k = \frac{-38,720}{4.575T}$$ ----------------------------------(13)

Thus, the apparent value for the activation energy for the oxidation of

iron in a mixture of CO_2 and CO is 38,720 calories. However, Benson[23]

described how the effect of very small errors in various experimental factors

can affect the value of the rate constant. Such small discrepancies can also

cause quite large errors in this value.

Weight Gain   To date, most of the kinetic data regarding the oxidation of

metals have been obtained by thermo-gravimetric (or Micro-balance) methods.

These, of course, are bulk oxidation procedures, since oxidation of the specimen

occurs on all exposed surfaces as contrasted with the linear oxidation on only one

exposed surface as in the current research.

$$\log R_f = 2.8 - \frac{38,720}{4.575T}$$
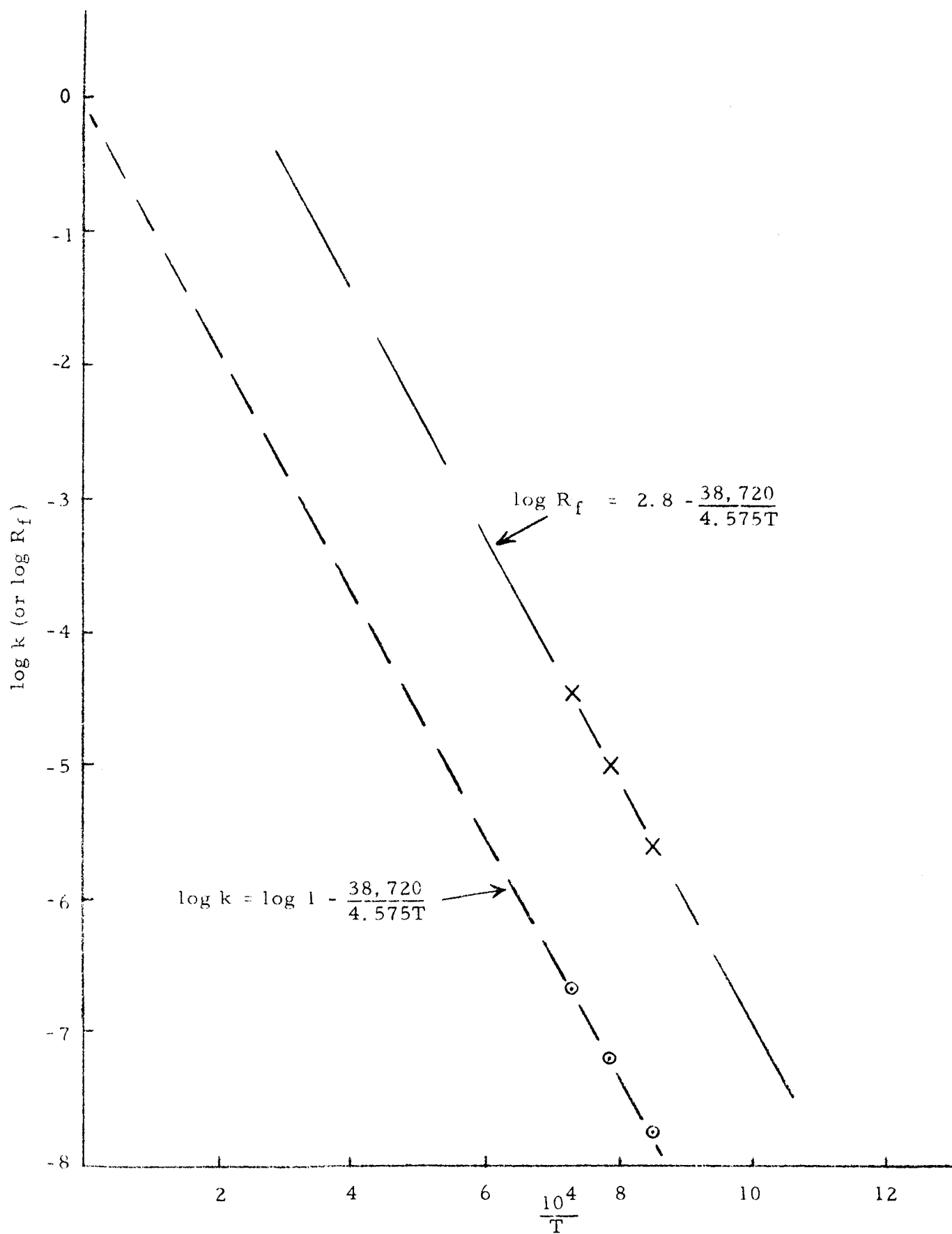
$$\log k = \log 1 - \frac{38,720}{4.575T}$$

Figure 8 Comparison of the Forward Reaction Rate with the Specific Rate Constant

However, the experimental data from the method used in the current

work can be translated into weight gain values. The weight of each specimen

is known and by assuming that the foils were transformed completely to wüstite

at point-C in the emf-time curve, the gain in weight of each specimen was

calculated. These results are shown in Table 2 and in Figure 9 where values

from experiments using a 5/1 ratio at 1000°C may be compared with the results of

Pettit and Wagner[17] who used a 1/1 ratio of CO_2/CO at 1100°C. Values from

the current work with a 5/1 ratio of CO_2/CO at 1000°C compare favorably with

Pettit and Wagner's results with a 1/1 ratio at 1100°C.

It has been pointed out by Pettit and Wagner[17] and others that the

oxidation of iron progesses from a linear to a parabolic rate after the oxide film

has progressed beyond a certain thickness. This is somewhat evident from the

trends shown in Figure 8. Kofstad[24] has suggested the term "general parabolic"

to describe this type of oxidation behavior. Such reactions are apparently

"interface controlled and linear during the initial stages and diffusion-limited

or parabolic after extended oxidation." According to Kofstad, this type of

behavior is described by the expression

$$x = k_p \frac{t}{x} - k_1 \quad\text{------------------------(14)}$$

and by plotting x vs t/x one may determine the parabolic rate k_p as the slope of

the line and k_1 as the intercept as $t/x = 0$.

PHASE I   SUMMARY AND CONCLUSIONS

The solid electrolyte technique which was proposed by Tare and

Schmalzried has been verified and has been developed into an effective and

useful tool for the determination of oxidation rates or iron.

Table 2 - Gain in Weight

| $\dfrac{CO_2}{CO}$	$t \ ^\circ C$	Foil Thickness (in.)	time	$\sqrt{t}$	$\dfrac{W}{A}\left(\dfrac{gms}{cm^2}\right) \times 10^3$
2/1	900	0.0004	360	19.0	0.90
"	"	0.0013	1380	37.2	2.90
"	"	0.0040	4200	65.0	8.96
"	"	0.0043	5700	75.5	9.65
5/1	"	0.0004	390	19.7	0.90
"	"	0.0010	1320	36.3	2.20
"	"	0.0013	1350	36.8	2.90
"	"	0.0013	1470	38.4	2.90
"	"	0.0040	4080	63.7	8.96
2/1	1000	0.0004	120	11.0	0.90
"	"	0.0004	120	11.0	0.90
"	"	0.0013	510	22.6	2.90
"	"	0.0040	1470	38.3	8.96
"	"	0.0043	1500	38.6	9.65
5/1	"	0.0004	120	10.9	0.90
"	"	0.0013	300	17.3	2.90
"	"	0.0040	1200	34.7	8.96
"	"	0.0043	1500	38.8	9.65
"	"	0.0050	1140	33.6	11.20
"	"	0.0055	1230	35.0	12.20
"	"	0.0069	1800	42.3	15.50
"	"	0.0082	2220	47.0	18.60
"	"	0.0085	2380	48.8	18.80
"	"	0.0095	2700	51.8	21.30
"	"	0.0096	3090	55.5	21.40
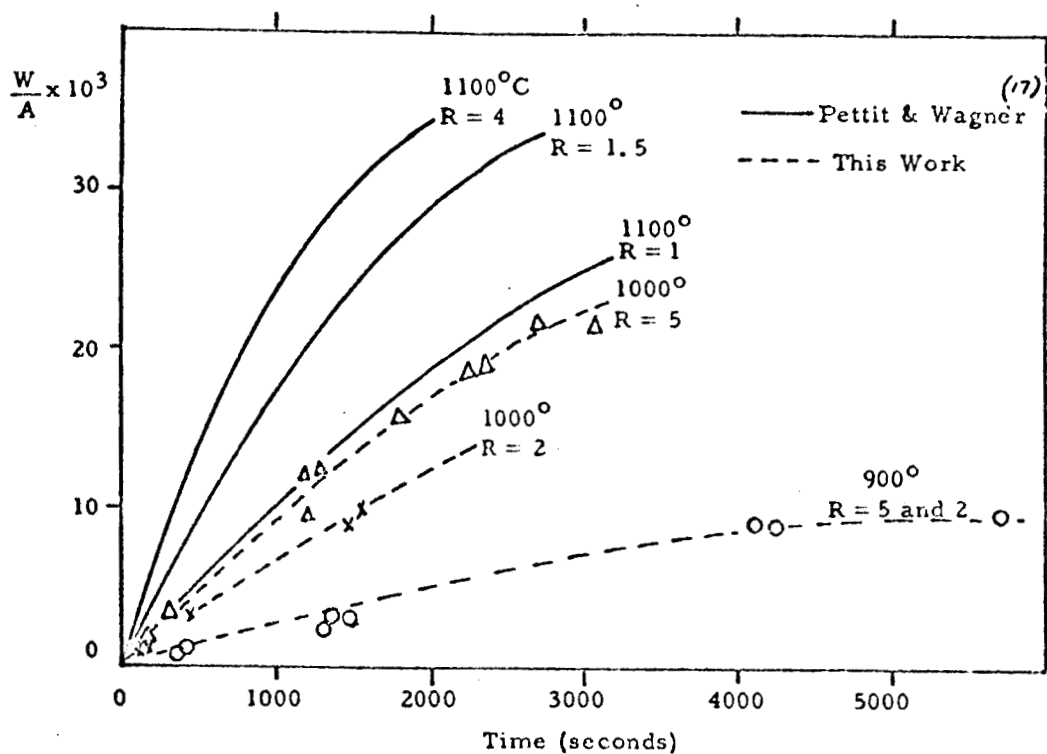
Figure 9   Weight Gain of Iron per cm^2 at Different Temperatures and CO_2/CO Ratios

In the current work, the linear rate constant proposed by these authors has been checked. In addition, the experimental data correlate reasonably well with the weight-gain method used by others for a study of the oxidation of iron to wüstite.

This work has verified the fact that the oxidation of iron in CO_2/CO atmospheres is linear at low oxide thicknesses, then becomes parabolic in thicker oxide films where the oxidation rate becomes diffusion controlled.

The solid electrolyte method promises to be quite useful in the determination of the oxidation kinetics of many steels because of its rapid response and the lack of need for high vacuum to prevent oxidation during the heating cycle.

The oxidation in this procedure progresses from only one surface at least in iron oxidation and is unique in this respect. Also, the cell voltage gives one a clue as to which oxide is being formed at various stages.

PHASE II OXIDATION OF NON-FERROUS METALS AND ALLOYS
(NICKEL AND NICHROME)

The application of a Tare and Schmalzried type cell to the study of
the rate of oxidation of pure iron was essentially a complete success.

Sufficient experimental data have been determined so that one can
predict with confidence the length of time for the complete oxidation of an
iron foil to wüstite if the thickness of the foil, the temperature and the
CO_2/CO ratio are specified. Such predictions were made in many of the
tests listed in Phase I. The results checked the predictions very closely.
Consequently, the initial studies of the oxidation of non-ferrous metals and
alloys were started with considerable confidence that similar results should
be obtained without alteration of the technique.

However, difficulties were encountered immediately. Regardless of
the temperature, the oxygen content of the gas, its flow rate or the surface
preparation of the foil, no characteristic oxidation curves were obtained. In
every case the cell voltage steadily decreased down to the equilibrium value
for the gaseous mixture as if the metal foil was not present. Some of the
early tests were listed in the October 1969 Progress Report and will not be
repeated here. The various parameters of these unsuccessful experiments on
nickel and nichrome are listed in the Appendix. An occasional iron specimen
was interspersed between the nickel and nichrome tests so as to be reassured
that the cell was operating properly.

Observation of the non-ferrous foils after these experiments indicated
that oxidation was taking place on both sides. This was the case even during

tests in which the foils were pressed against the surface of the electrolyte tube with considerable pressure. This had not been the case with iron foils which oxidized linearly from one side. The oxidation of iron to wüstite is not a diffusion controlled process until thick foils are used, but this is not the case with nickel and nichrome.

New Cell Design   In view of the above difficulties, the cell was redesigned as in Figure 10 so as to eliminate the C-circuit shown in Figure 4. In addition, the revised cell provided an argon atmosphere around the outside of the electrolyte tube except at the end with the foil. In this manner the CO_2/CO mixture impinged directly on the end of the tube and the foil. In addition, the foil was pressed against the end of the electrolyte tube by the spring mechanism which was mentioned previously.

These changes did not alter the oxidation characteristics of nickel or nichrome. The oxidation occurred on both sides of the foils and failed to indicate any of the thermodynamic "plateau's" or trends which would be characteristic of a known oxide. Instead the voltage dropped directly to that of the gaseous equilibrium in each case.

OXIDATION OF MOLYBDENUM

The free energy of formation of molybdenum dioxide (MoO_2) is of the same order of magnitude of that for wüstite. For this reason it was decided to study the oxidation of molybdenum and the results, as shown in Table 4 of the Appendix were similar to those for nickel and nichrome.
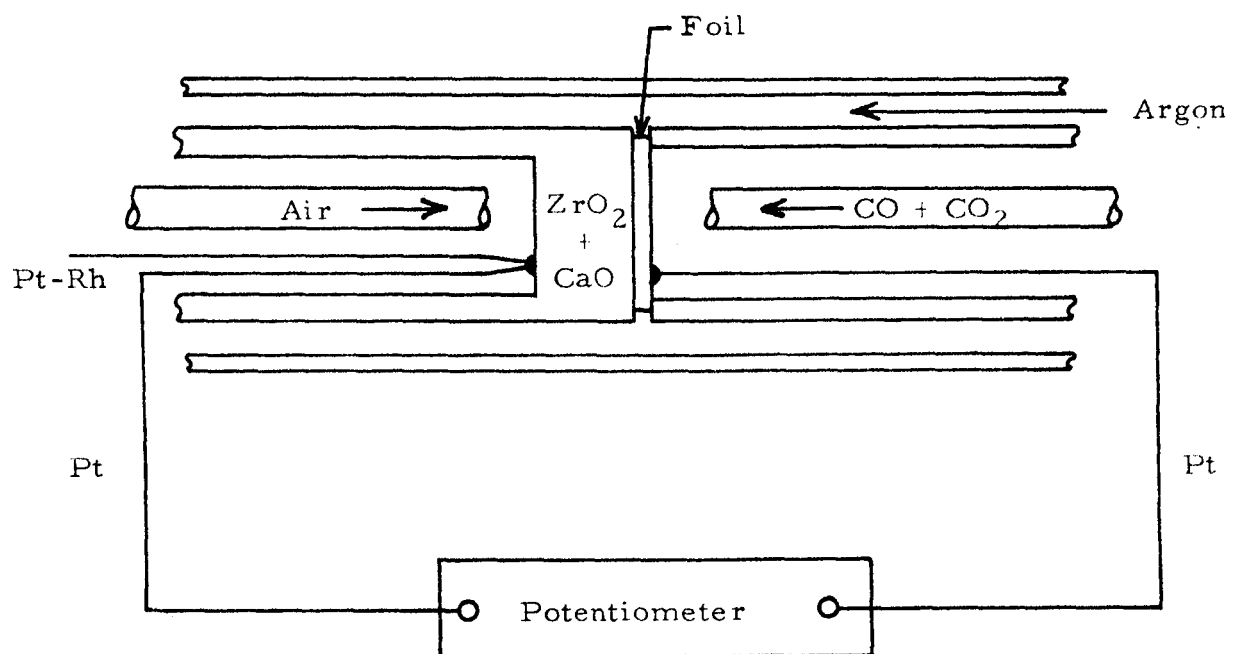
Figure 10.   THE RECONSTRUCTED CELL

Experiments were made using both the old and the new cells without success. Care was taken in all such experiments to maintain a neutral atmosphere until the cell and foil had attained the experimental temperature. In fact, numerous experiments were made in which the system was heated to, and cooled from, the experimental temperatures in the neutral atmosphere to determine if any oxidation took place during the heating cycle. It was determined that no such oxidation occurred. However, in every case oxidation occurred on both sides of the foil when the oxidizing CO_2/CO mixtures were used.

<u>The Foil-Electrolyte Contact</u>   These difficulties all pointed to the possible poor contact between the foil and the end of the electrolyte tube. Tare and Schmalzried had predicted some difficulty which would originate from poor contact. For some reason the contact was sufficient in every experiment involving iron foil but was entirely inadequate for the non-ferrous metals and alloys. No amount of care in surface preparation of the foil and/or the electrolyte or excessive pressures of the foil against the electrolyte were helpful.

Several experiments were next made in which the end of the electrolyte tube was first coated with a deposit of pure molybdenum by means of an electron beam gun. Although the thickness of the deposit was not measured, previous experience with the electron beam unit indicated similar deposits in other types of experiments ranged from 3000 to 5000 $\overset{O}{A}$ in thickness.

The molybdenum foil was then mounted in the cell against the molybdenum deposit under pressure as in the revised cell. Experiments conducted in this manner produced trends similar to those exhibited by iron.

Figure 11 is a tracing of one such successful experiment in which the molybdenum was oxidized at 1000°C with a CO_2/CO ratio of 5/1. A copy of the original record is shown in the Appendix.

In this experiment the cell was heated to 1000°C in an atmosphere having a CO_2/CO ratio of 0.32 which was calculated to be slightly reducing with respect to molybdenum. During this period the cell voltage stabilized at 910 millivolts. This is shown in the original record as point-A.

The CO_2/CO ratio was then suddenly changed to 5/1 and the cell voltage fluctuated as shown in the figure. As a first approximation it may be assumed that the formation of MoO_2 was quickly nucleated at point-B and that the foil had been completely oxidized to MoO_2 at point-C. Following this the MoO_2 was partially oxidized to MoO_3 with a further decrease in voltage and a leveling-off or a "plateau" at point-D. From this point on the EMF continued to decrease until that of the gaseous reaction was reached.

THERMODYNAMIC ANALYSIS

Oxidation to MoO_2 According to Kubaschewski, Evans and Alcock[13] the free energy of formation of molybdenum dioxide may be expressed as,

$$\triangle G° = -149,100 - 4.6\, T\log T + 55.8\, T \text{ for } Mo + O_2 = MoO_2 \quad \text{------(15)}$$
$$\text{and at } 1000°C \ (1273°K), \ \triangle G° = -87,251 \text{ calories}$$

The reaction free energy may be included in the cell free energy equation, in a manner similar to that for wüstite in Equation-6, or
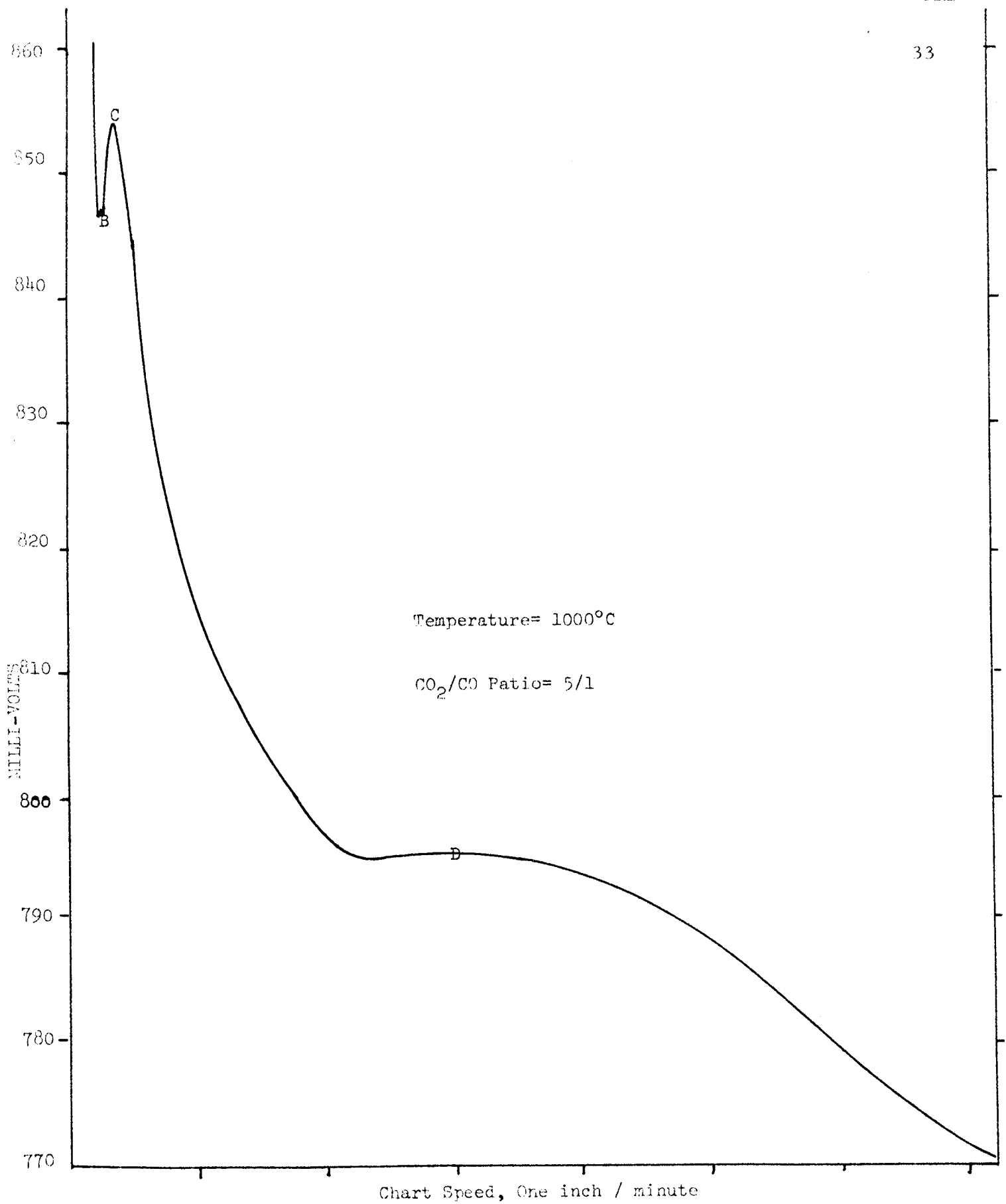
Figure 11 Oxidation of Pure Molybdenum Foil

$$\Delta G_R = -neF - \Delta G^o + 2RT \ln CO_2/CO \quad ----------------------(16)$$

$$= -87,251 + 9.15 (1273)(0.7)$$

$$= -79.097$$

$$e = \frac{79,097}{92,264} = 0.857 \text{ volts, since } n = 4$$

The peak at point-C in Figure 11 occurred at 854 milli-volts, which is a remarkable check of the thermodynamically calculated value. This peak was arrived at in twelve seconds, thus indicating a very rapid reaction for the formation of MoO_2. Further it is evident from the shape of the curve A-B-C, that the oxidation of molybdenum to MoO_2 is nucleated in a manner which is quite similar to that for wüstite.

Indication of MoO_3 Formation   After reaching its peak, the voltage continued to decrease for about two minutes and then leveled off at a "plateau" at point-D. This plateau occurred at 795 millivolts in about 190 seconds but the significance of this trend was not immediately understood.

It may be rationalized that the rate of diffusion of oxygen into the metal foil is slow relative to the rate of oxidation of molybdenum to MoO_2 at the surface of the foil. Further, it will be assumed here that the principal reaction of the metal with these gases at 1000^oC involves its oxidation to the dioxide.

However, as the dioxide forms it is conceivable that it is further oxidized at the gas-oxide interface to MoO_3. This procedure would continue until either the metal foil had been completely oxidized or a thick oxide impervious film had formed.

Thus, the potential of the cell at point-D would be determined by the effect of the formation of MoO_3 on the free energy of formation of MoO_2.

Thermodynamic calculations may be made by assuming this sequence of reactions as an hypothesis. Further, the effect of the CO_2/CO ratio on the formation of the trioxide must be treated consistently as in the case of wüstite, in Equation-6 and in the case of the dioxide in Equation-16.

Thus, the reaction for the formation of MoO_3 from MoO_2 and oxygen, is

$$MoO_2 + 1/2\ O_2 = MoO_3 \quad \text{------------------------------(17)}$$
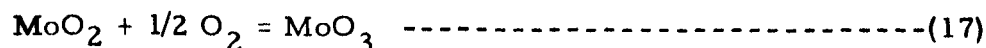
However, the reaction free energy in the presence of CO_2 and CO would be

$$\triangle G_R = \triangle G^o_{17} + RT\ \ln\ \frac{CO_2}{CO} \quad \text{--------------------------(18)}$$

It must now be assumed again that the cell potential is largely the result of the MoO_2 formation under the conditions of this cell reaction and that the formation of MoO_3 detracts from that potential. Thus, during the formation of MoO_3,

$$\triangle G_R = -neF = \triangle G_R\ (16) - \triangle G_R\ (18) = \triangle G^o_{15} - \triangle G^o_{17} + RT\ln\frac{CO_2}{CO}\ \text{--(19)}$$

As shown previously,

$$\triangle G^o_{15} = -87,251 \quad \text{calories at } 1000^\circ C.$$

Further, the standard free energy[13] for the formation of MoO_3 from MoO_2 and oxygen (Reaction-17) is

$$\triangle G^o_{17} = -38,700 + 19.5\ T \quad \text{----------------------------------(20)}$$

and at $1273^\circ K$, $\triangle G^o_{17} = -13877$ calories.

Thus the cell potential during the formation of MoO_3 under these conditions should be

$$e = -\ (\frac{\triangle G^o_{15} - \triangle G^o_{17} + RT\ \ln\ \frac{CO_2}{CO}}{nF})$$

$$= -\ (\frac{-87,251 + 13,877 + 4077}{92,264}) = 0.751\ \text{volts}$$

It should be recalled that since the principal reaction involved here is the oxidation of molybdenum to the dioxide, the value of n = 4

The actual cell potential at point-D in Figure 11 was 795 milli-volts. In the second experiment as shown in Figure 2 of the Appendix, the curve did not exhibit a plateau but a break in the curve occurred at 798 milli-volts. However, the effect was not sustained. Thus the above calculation is within 5.5% of the experimental results. As stated previously, the cell voltage continued to drift downward after the "plateau" was exhibited until it reached a value of 756 milli-volts which approximates the potential of the gaseous reaction as expressed in Equation-2.

If one may accept this concept for the combined reactions, the following explanation may be postulated for the reaction mechanism.

At the end of each experiment the foils were examined and in every case a thick tenacious MoO_2 film had formed on the surface but considerable metallic foil remained.

It is possible that during the early stages of oxidation that diffusion processes are rapid enough to permit the oxide film to develop to a certain critical thickness. However, it is conceivable that when this thickness is reached the molybdenum ion diffuses more rapidly to the oxide surface than the oxygen ion can diffuse through the oxide film to form MoO_2 at the metal-oxide interface.

When this stage is reached the gases tend to oxidize some of the dioxide to the trioxide. However, because of the diffusion of the metal ion through the oxide film the dioxide is reformed.

Finally, the oxide film becomes so thick that the transport of the metal ion to the gas-oxide surface is insufficient to sustain the reaction involving the tri-oxide. However, some of the dioxide may be oxidized to trioxide at the gas-oxide surface. If so the trioxide which will form readily up to very high temperatures would evaporate and cease to influence the cell potential. It is well known that the trioxide melts at about $800^{\circ}C$ but vaporizes readily at higher temperatures.

CONCLUSIONS, PHASE II

The experiments on the oxidation characteristics of both iron and molybdenum present considerable promise that this method can provide accurate and useful information regarding the oxidation of metals and alloys.

This is particularly the case if the metallic contact with the electrolyte is insured by first depositing some of the metal on the end of the electrolyte tube.

If the oxidation of the metal or alloy is not diffusion controlled, good kinetic data can be obtained and basic thermodynamic data may be used to determine which oxides are forming at any instant.

Analysis of the thermodynamic data obtained by this method provides considerable insight into the mechanism of oxidation which cannot be determined by any other technique.

This experimental procedure should be investigated further so as to provide knowledge concerning the various mechanisms of oxidation of metals and alloys particularly those which exhibit more than one oxide.

The oxidation characteristics of most steels could be studied thoroughly by this method. Further, metals whose oxides have larger standard free energies of formation(or lower oxygen pressures) than wüstite may be studied using calcia

stabilized zirconia as the electrolyte as shown in Figure 12. Some metals having more stable oxides than those shown in this chart may conceivably be studied using yttria stabilized thoria electrolyte tubes.
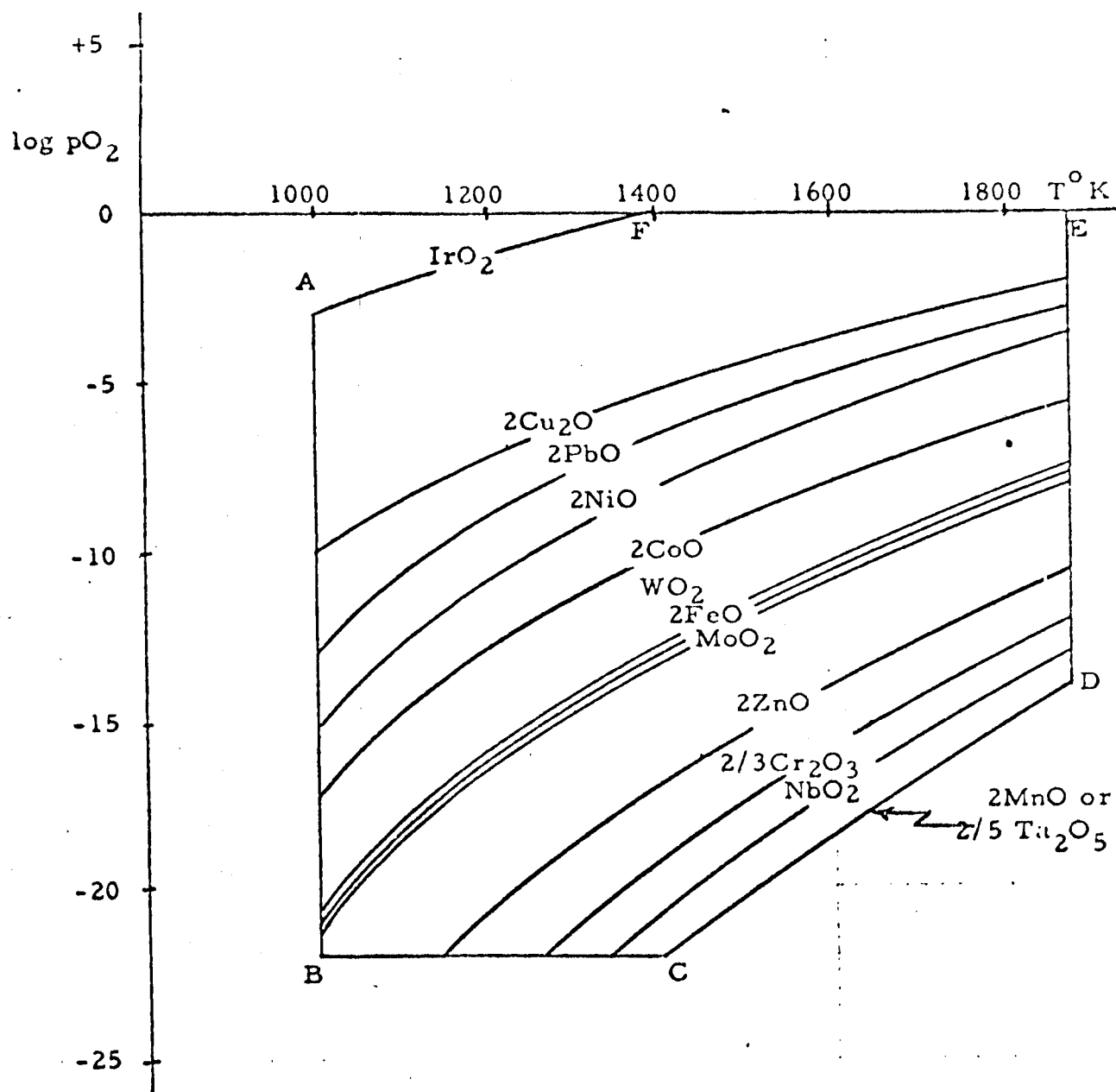
Figure 12 Estimated Limits of Application
of the Calcia-Stabilized Zirconia Electrolyte
Using Pure O_2 as the Reference State

APPENDIX

TABLES

FIGURES

Table 1   OXIDATION STUDIES OF NICKEL

A.   COLD ROLLED

Foil Thickness Inches	Temp. $^{\circ}C$	Oxidizing Atomosphere
.010	1200	O_2
.010	1000	O_2
.010	1000	Air
.010	1100	$O_2/A = 0.1$
.010	1100	$O_2/A = 0.1$
.010	1100	O_2

B.   COLD ROLLED, AND VACUUM ANNEALED

.010	1100	O_2

C.   COLD ROLLED, VACUUM ANNEALED & ETCHED

.009	1100	O_2
.009	1100	O_2 200 ma thru cell

D.   LEVITATION MELTED

.0025	1100	O_2
.002	1100	O_2 1 ma thru cell

Table $\underline{2}$ OXIDATION STUDIES OF NICKEL-CHROMIUM ALLOYS

COLD ROLLED NICHROME

Foil Thickness Inches	Temp. ^{o}C	Oxidizing Atmosphere	
.002	1000	$CO_2/CO = 10$	
.002	1000	$CO_2/CO = 8$	
.002	1100	O_2	

COLD ROLLED AND VACUUM ANNEALED NICKROME

.002	1100	O_2	
.002	1100	O_2	
.002	1100	O_2	Protected by back emf until oxidized.
.002	1100	O_2	External pressure applied
.002	1100	O_2	Sauereisen cement to hold foil in place

COLD ROLLED, VACUUM ANNEALED AND ETCHED NICHROME

.002	1100	O_2	
.002	1100	O_2	

LEVITATION MELTED 50 $^{A}/_{O}$ Cr - 50 $^{A}/_{O}$ Ni

.002	1100	O_2	External Pressure Applied

Table $\underline{3}$ OXIDATION STUDIES OF IRON

A.   COLD ROLLED

Foil Thickness Inches	Temp. $^{\circ}$C	Oxidizing Atmosphere	
.0004	900	$CO_2/CO = 1.0$	Double Atm.
.0004	1000	$CO_2/CO = 2.0$	Double Atm.
.004	1000	$CO_2/CO = 5.0$	Double Atm.
.004	1000	$CO_2/CO = 5.0$	Double Atm.
.004	1000	$CO_2/CO = 5.0$	

B.   COLD ROLLED STAINLESS STEEL

.002	900	$CO_2/CO = 1.0$	

C.   VAPOR DEPOSIT OF IRON ON END OF ZIRCONIA TUBE

.0004	900	$CO_2/CO = 2.0$	(Normal run for Fe)

Table 4 OXIDATION STUDIES OF MOLYBDENUM

A. COLD ROLLED

Foil Thickness Inches	Temp. °C	Oxidizing Atmosphere	
.010	900	$CO_2/CO = 2.0$	
.005	900	$CO_2/CO = 1.0$	
.005	900	$CO_2/CO = 1.0$	Sauereisen cement to seal foil to tube
.005	900	$CO_2/CO = 1.0$	
.005	900	$CO_2/CO = 1.0$	
.005	900	$CO_2/CO = 2.0$	
.005	900	$CO_2/CO = 2.0$	
.005	900	$CO_2/CO = 2.0$	
.005	1000	$CO_2/CO = 5.0$	
.005	1000	$CO_2/CO = 5.0$	
.005	1000	$CO_2/CO = 2.0$	Double Atm.
.005	1100	$CO_2/CO = 5.0$	Double Atm.
.005	1200	$CO_2/CO = 2.0$	Double Atm.
.005	1200	$CO_2/CO = 2.0$	Double Atm.

B. ELECTRON BEAM VAPOR DEPOSITED FILM OF MOLYBDENUM ON END OF ELECTROLYTE TUBE

0.005	900	$CO_2/CO = 5.0$
0.005	1000	$CO_2/CO = 5.0$
0.005	1000	$CO_2/CO = 5.0$

10 mw BLUE SCALE, $t \, ^\circ C$

D

C

B

A

$CO_2/CO = 0.32 \rightarrow 5/1$

$t = 1000 \, ^\circ C$

FIGURE 1. 5 MIL Mo   Mo - VAPOR DEPOSITED
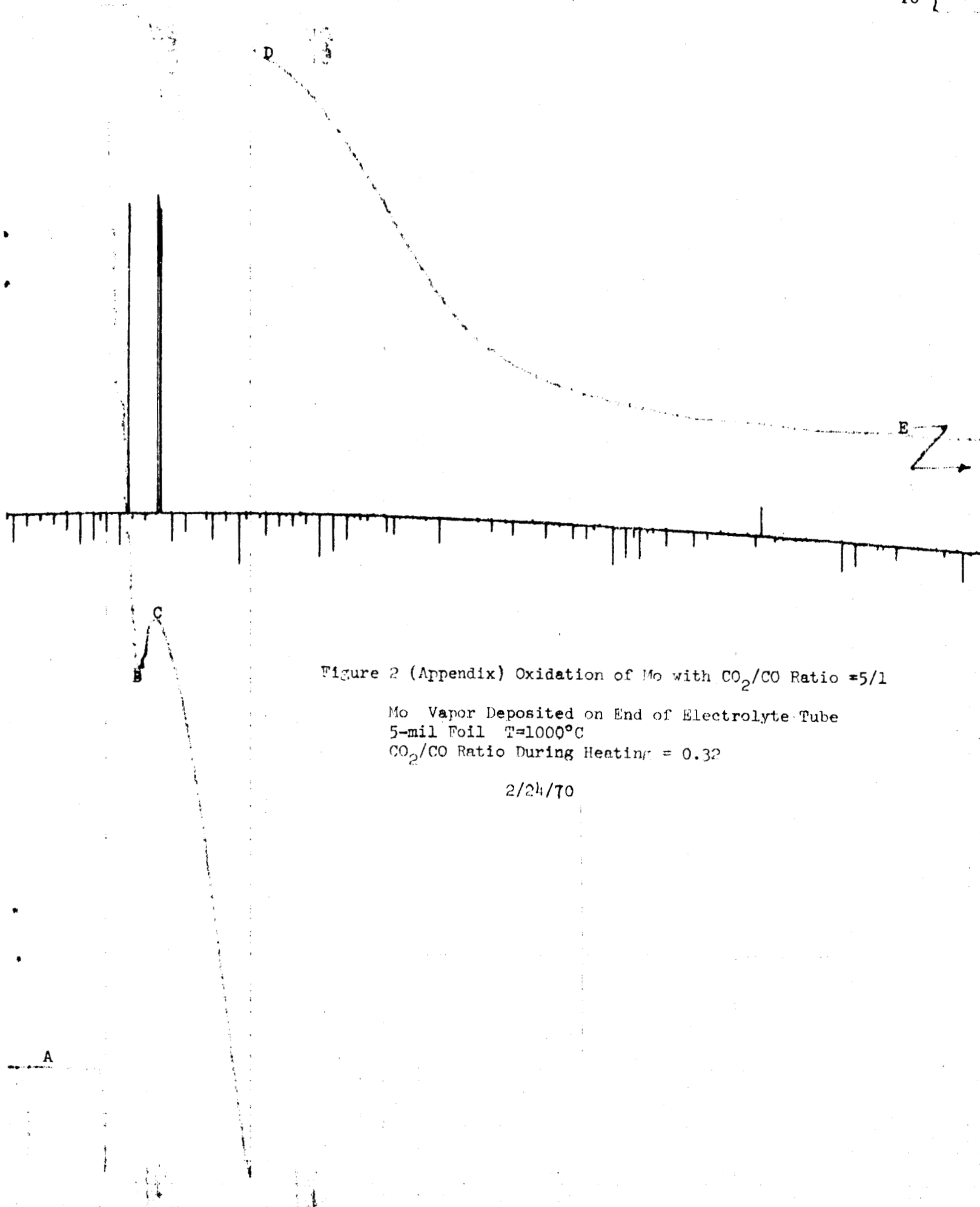(APPENDIX)   ON ZIRCONIA TUBE

2/20/70

1"/MIN.
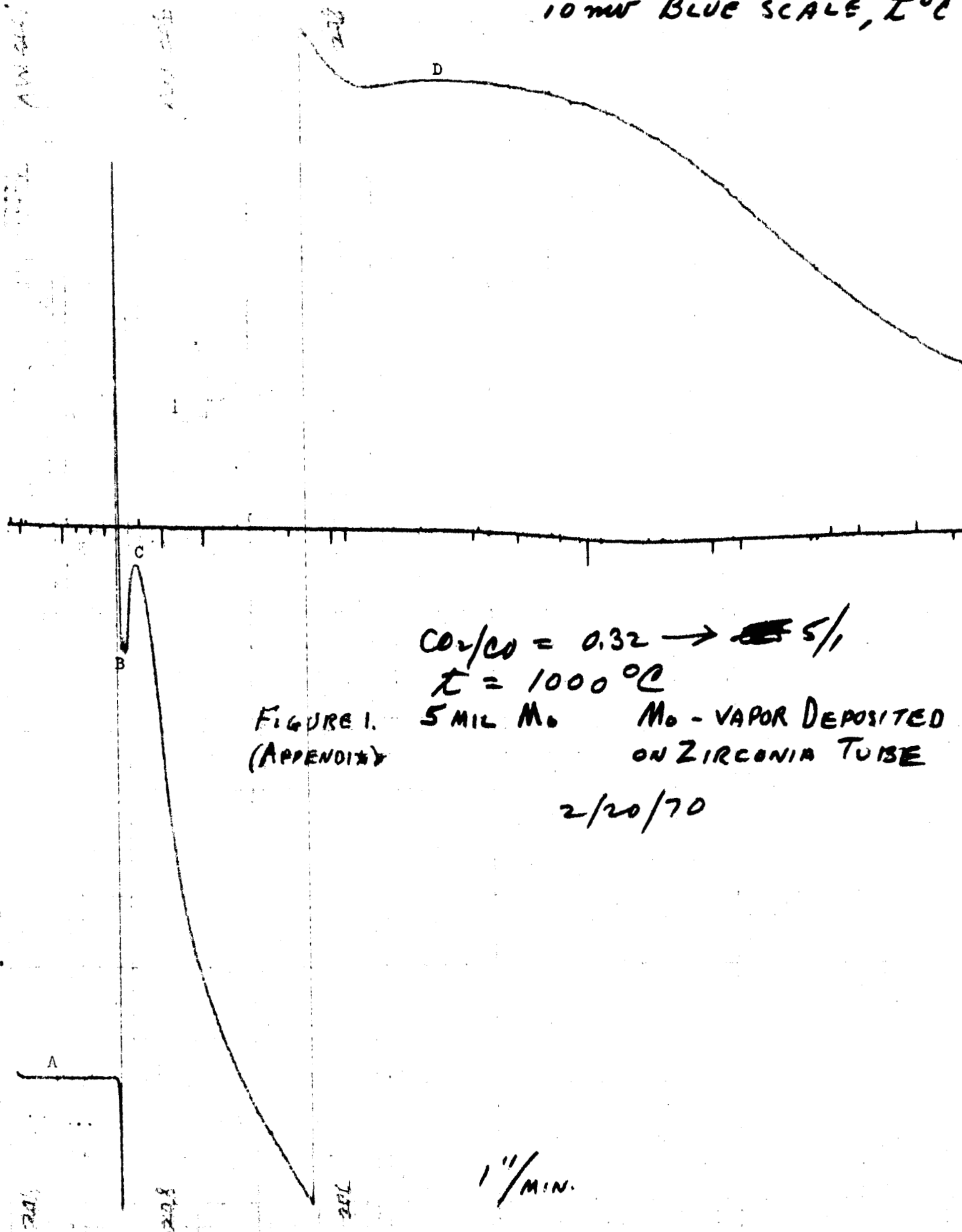
Figure 2 (Appendix) Oxidation of Mo with CO_2/CO Ratio $= 5/1$

Mo   Vapor Deposited on End of Electrolyte Tube
5-mil Foil   T=1000°C
CO_2/CO Ratio During Heating = 0.32

2/24/70

BIBLIOGRAPHY

1. K. Kiukkola and C. Wagner, J. Electrochem. Soc., 104, 379, 1957

2. Y. Matsushita and K. Goto, Thermodynamics Conference, IAEA, 1, 111, Vienna, 1966.

3. W. L. Worrell, ibid., p. 131

4. G. B. Barbi, J. Phys. Chem., 68, (5), 1025, 1964

5. R. A. Rapp and F. Maak, Acta Met., 10, 63, 1962

6. K. Schwerdtfeger and A. Muan, Acta Met., 13, 509, 1965

7. R. J. King and G. R. Fitterer, Pt-Co System. Presented at the AIME Institute of Metals Meeting, Pittsburgh, May, 1969

8. L. A. Pugliese and G. R. Fitterer, The Cr-Ni System, ibid.

9. H. Rickert, Electromotive Force Measurements in High Temperature Systems Symposium, C. B. Alcock, ed., American Elsivier Publishing Co., 1968

10. F. C. Arcella and G. R. Fitterer, Diffusion of Oxygen in Liquid Lead, Presented at the AIME Annual Meeting, Washington, D. C., Feb., 1969

11. V. B. Tare and H. Schmalzried, Trans. AIME, 236, 444, 1966

12. L. S. Darken and R. W. Gurry, J. Am. Chem. Soc., 67, 1398, 1945

13. O. Kubaschewski, E. L. Evans and C. B. Alcock, Metallurgical Thermochemistry, 4th ed., Pergamon Press, 1967

14. H. Rizzo, Thermodynamics of the Fe-O System, Ph. D. Thesis, University of Utah, 1968

15. G. L. Humphrey, E. G. King and K. K. Kelly, U. S. Bureau of Mines R. I. 4870, 1952

16. H. Kubayashi and C. Wagner, J. Chem. Phys., 26, (6), 1609, 1957

17. F. S. Pettit and J. B. Wagner, Acta. Met., 12, 35, 1964

18. H. A. Taylor, J. Phys. Chem., 34, 2761, 1930

19. H. J. Grabke, Berichte der Bunsengeselschaft, 69, (1), 46, 1965

20. W. A. Edmiston and R. E. Grace, Trans. AIME, 236, 1547, 1966

21. I. Prigogine, P. Outer and C. Herbo, J. Phys. and Colloid Chem., 52, 321, 1948

22. M. Manes, L. J. E. Hofer and S. Weller, J. Chem. Phys., 18, 1355, 1950

23. S. W. Benson, "The Foundations of Chemical Kinetics," McGraw Hill, 1960

24. Per Kofstad, "High Temperature Oxidation of Metals," John Wiley and Sons, 1966

Research Grant NGR 39-011-067

Adressee	Number of Copies

(1) NASA Headquarters
Washington, D. C. 20546
Attention: N. F. Rekos (RAP)   1
G. C. Deutsch (RRM)   1

(2) NASA Lewis Research Center
21000 Brookpark Road
Cleveland, Ohio 44135
Attention: Technology Utilization Office (MS 3-19)   1

(3) NASA Lewis Research Center
21000 Brookpark Road
Cleveland, Ohio 44135
Attention: Materials and Structures Division
G. M. Ault (MS 105-1)   1
R. W. Hall (MS 105-1)   1
N. T. Saunders (MS 105-1)   1
Dr. H. B. Probst (MS 49-1)   1
Dr. I. Zaplatynsky (MS 49-1)   2
S. J. Grisaffe (MS 49-1)   1
Dr. J. S. Wolf (MS 49-1)   1
C. E. Lowell (MS 49-1)   1
R. E. Oldrieve (MS 105-1)   2
A. E. Anglin (MS 105-1)   1

(4) NASA Lewis Research Center
21000 Brookpark Road
Cleveland, Ohio 44135
Attention: Airbreathing Engines Division
J. Howard Childs (MS 60-4)   1

(5) FAA Headquarters
800 Independence Avenue, S. W.
Washington, D. C. 20553
Attention: Brig. Gen. J. C. Maxwell   1
F. B. Howard SS/120   1

(6)   Defense Metals Information
Battelle Memorial Institute
505 King Avenue
Columbus, Ohio 43201   1

(7)   Central Institute for Industrial Research
Oslo, Blindern, Norway
Attention: Dr. Per Kofstad   1

(8)   Metallurgical Laboratories
University of Clausthal
Clausthal, West Germany
Attention: Dr. Hermann Schmalzried, Director   1

(9)   University of Pennsylvania
34 th and Spruce Streets
Philadelphia, Pennsylvania 19104
Attention: Dr. V. B. Tare   1